

# Different techniques of alumina film deposition

Zhihong Zhao (赵志宏), Yiqin Ji (季一勤)\*, Dandan Liu (刘丹丹), and Jie Zong (宗杰)

Tianjin Key Laboratory of Optical Thin Films, Institute of Jinhang Technical Physics, Tianjin 300192, China

\*E-mail: ji-yiqin@yahoo.com

Received December 8, 2009

$\text{Al}_2\text{O}_3$  films are deposited using ion beam sputtering (IBS), ion beam reactive sputtering (IBRS), and electron beam evaporation (EBE). The properties of the films, such as optical identity, surface roughness, microstructures, and crystalline phase, are investigated. The single layer of alumina is discussed using the IBS method. It has a high refractive index and a perfect microstructure as well as a high ultraviolet (UV) absorption. The roughness of the  $\text{Al}_2\text{O}_3$  film deposited using EBE is larger than that of the substrate surface, but it is in an acceptable range. The film deposited using EBE is dominated by the amorphous gamma phase, while the ones deposited using IBS and IBRS are an intermixture of the alpha alumina and the gamma alumina phases.

OCIS codes: 100.6640, 210.4770, 180.1790.

doi: 10.3788/COL201008S1.0083.

Alumina films are widely used in the fields of optics, mechanics, micro-electronics, chemistry, due to their excellent properties in terms of transmittance, hardness, chemical inertness, and resistivity<sup>[1,2]</sup>. As a kind of optical coating material with a high transmittance in the range from the ultraviolet (UV) to infrared (IR) band, alumina is popularly used as a material with high refractive index in the UV and visible (VIS) ranges and with low refractive index in the IR range.

Electron beam evaporation deposition (EBED) and ion beam sputtering deposition (IBSD) are two popular techniques used for alumina coating deposition. EBED, which depends on the thermal electron emission of a high temperature metal filament heating up and gasifying the coating materials, is the most advanced coating technique. IBSD, on the other hand, is achieved by a momentum exchange; that is, high speed ions sputter out the target particles directly. There are two ways of depositing alumina coatings using the ion beam sputtering (IBS) mode. One is that the ion beam sputters the  $\text{Al}_2\text{O}_3$  target directly, the other has the IBS the Al target in an oxygen atmosphere, which is called the ion beam reactive sputtering deposition (IBRSD). The properties of the coatings deposited using EBED, IBSD, and IBRSD are discussed in this letter.

Three groups of samples were coated on substrates of

fused silica and silicon in each group by the use of EBED, IBSD, and IBRSD, respectively. The details of the manufacturing process are given in Table 1.

The optical characteristics were determined based on the measured spectral curves. A Perkin Elmer Lambda 900 UV/VIS/NIR spectrometer, a Perkin Elmer FT-IR Spectrum GX spectrometer, and a variable angle spectra ellipse (VASE) were used. A Zygo NewView 5000 surface structure analyzer was used to measure the coating roughness. Scanning electron microscope (SEM) measurements were performed at the Fudan University.

The refractive index curves of the sample films fitted using VASE is shown in Fig. 1. In agreement with our assumption, the refractive indices of samples 1 and 2 are obviously higher. The incident energy of the particles sputtered out from the target, which is 100 times higher than that of the evaporated particles, is high enough to make the particles continue moving after they arrive at the surface of the substrate. The higher refractive index is achieved by the particle movement on the surface, which reduces the lacuna of the coatings and makes the coatings more compact. Compared with sapphire<sup>[3]</sup>, the alumina coatings deposited using IBSD and IBRSD have the refractive indices 90% higher than that of the bulk material.

Once the hypothesis about the gradual change in

Table 1. Manufacturing Details

| Technique | Parameters                     | Substrate            | Sample Number | Thickness of Film (nm) |
|-----------|--------------------------------|----------------------|---------------|------------------------|
| IBSD      | Beam Current 300 mA            | $\text{SiO}_2$<br>Si | 1#            | 460                    |
|           | Beam Voltage 1000 V            |                      |               |                        |
|           | Room Temperature               |                      |               |                        |
| IBRSD     | Beam Current 300 mA            | $\text{SiO}_2$<br>Si | 2#            | 735                    |
|           | Beam Voltage 1000 V            |                      |               |                        |
|           | Room Temperature               |                      |               |                        |
|           | Ar:O <sub>2</sub> =0.8         |                      |               |                        |
| EBED      | Deposition Rate 0.45 nm/s      | $\text{SiO}_2$<br>Si | 3#            | 572                    |
|           | Pressure $2 \times 10^{-3}$ Pa |                      |               |                        |
|           | Substrate Temperature 250 °C   |                      |               |                        |

**Table 2. Change of MSE**

| Hypothesis           | MSE      |          |          |
|----------------------|----------|----------|----------|
|                      | Sample 1 | Sample 2 | Sample 3 |
| nf is invariable     | 5.570    | 4.781    | 7.554    |
| nf changes gradually | 1.568    | 4.768    | 4.966    |

nf: refractive index of the film

the refractive index of the coating is taken into account, it diminishes the MSEs of VASE fitting to samples 1 and 3 (Table 2). Hence, it is inferred that the refractive indices of samples 1 and 3 become higher during the growing process. The region of disturbed plasma near the Al<sub>2</sub>O<sub>3</sub> target, the so-called sheath<sup>[4]</sup>, is presumed to be built during the deposition process of sample 1 because the positive charges transported by Ar<sup>+</sup> accumulate on the surface of the dielectric Al<sub>2</sub>O<sub>3</sub> target and cannot be completely neutralized by the neutralizer. The most important characteristic of the sheath is the local electric field, which is responsible for the disturbance of the plasma near the target and the gradual change of the coating refractive index caused by decreasing the deposition rate. Compared with the alumina target, the aluminum target is conductive and no sheath is formed. Hence, sample 2 has a steady refractive index. In the experiments, SiO<sub>2</sub> coatings are deposited with a SiO<sub>2</sub> target and Ta<sub>2</sub>O<sub>5</sub> coatings are deposited with a Ta target, a gradual change in SiO<sub>2</sub> coating and the steady Ta<sub>2</sub>O<sub>5</sub> coating are also observed.

For the EBED process, islands are formed at the start of the deposition process because of less saturation between the alumina and the substrates. The lower energy of the transport particles limits the particle movements between the islands, and more lacunas are produced. However, the alumina deposited is saturated with the former coating, which leads to fewer lacunas and higher compactness as well as higher refractive index.

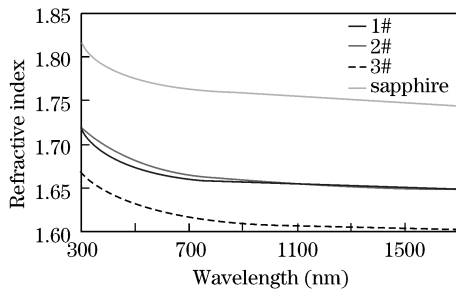


Fig. 1. Refractive index of sapphire and the fitted sample refractive indices.

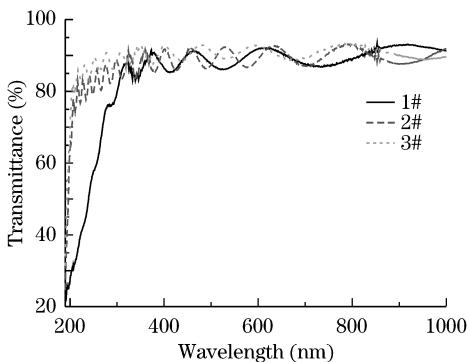


Fig. 2. Transmittance of the samples.

The transmittances are determined using a Lambda 900 UV/VIS/NIR spectrometer (see Fig. 2) and the extinction coefficients of the samples are calculated using the envelope method<sup>[5]</sup> (see Fig. 3). The extinction coefficient of sample 1 increases dramatically at the UV range but it has the lowest value in the near-infrared (NIR) range. On the other hand, sample 3 has the lowest extinction coefficient in the NIR range. The extinction coefficient increases a little in the VIS range and slopes gradually in the NIR range. Based on the theory of dispersion<sup>[6]</sup>, dispersion will be induced while light-wave passes through an irregular medium. Thus, the

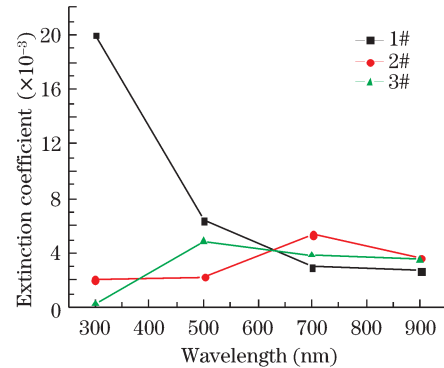


Fig. 3. Calculated extinction coefficient of the samples.

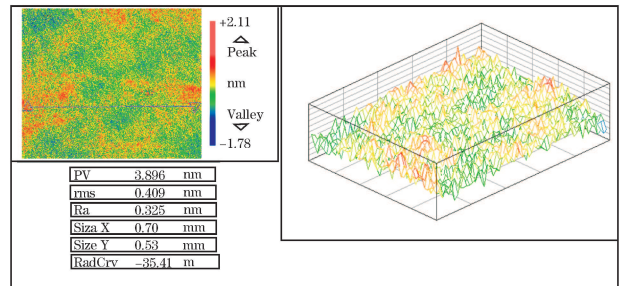


Fig. 4. Surface map of sample 1.

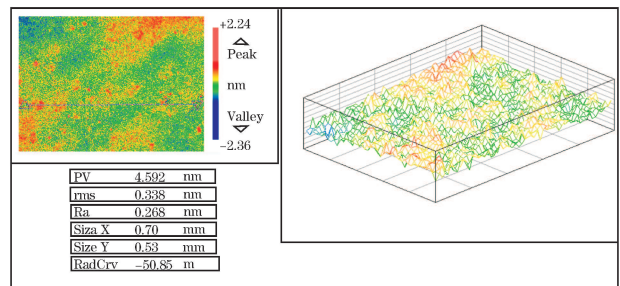


Fig. 5. Surface map of sample 2.

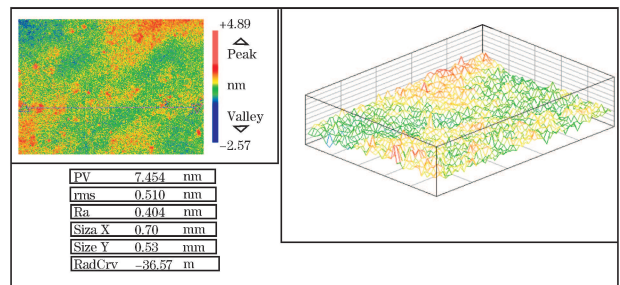


Fig. 6. Surface map of sample 3.

absorption of sample 1 in the UV region is considered to be a result of dispersion inside of the film. According to Ref. [7], low absorption can be achieved with lower ion beam power.

The surface maps of the coatings on the fused silica substrate with root mean square (RMS) of roughness within 0.5 nm are constructed using a Zygo NewView 5000 surface structure analyzer (Figs. 4–6).

As expected, samples 1 and 2 have lower roughness values. The powerful kinetic energy of the sputtered particles makes them move on the substrate surface, in turn, it reduces the lacunas in the coating and even re-makes the substrate surface. Hence, samples 1 and 2 have lower roughness values than that of the substrates even. However, the lower energy of the evaporated particles cannot improve the coating roughness and instead leads to larger peak-to-valley (PV) value. The roughness of sample 3, on the other hand, does not match the value described in Ref. [8] because it does not rise sharply. This may be due to the difference in the roughnesses of the substrates. It is a fact that the coatings magnify the lacunas on the substrate surface because particles transported using EBED do not have enough energy to move on the surface of the substrate and reunite more easily near the lacunas than on smooth surface. Hence, the roughness of the substrate surface is considered to be responsible for the roughness of the coatings deposited using EBED.

The microstructures of the coatings are observed by SEM, as shown in Fig. 7. The characteristics of the three samples are not obvious, matching the results mentioned above.

The microstructures of the coating sections show different structures in Fig. 8. The most compact coating of sample 1 makes its characteristics inconspicuous, but a distinct combination layer is formed by the powerful ion beam between the coating and the substrate. Little granules can be observed in sample 2 but there is no combination layer present. The differences in deposition method and ion beam power cause the diversities

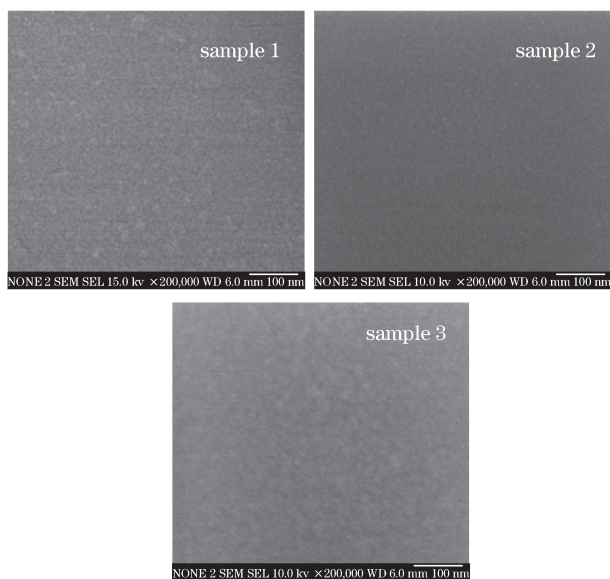


Fig. 7. Microstructures of the sample surfaces.

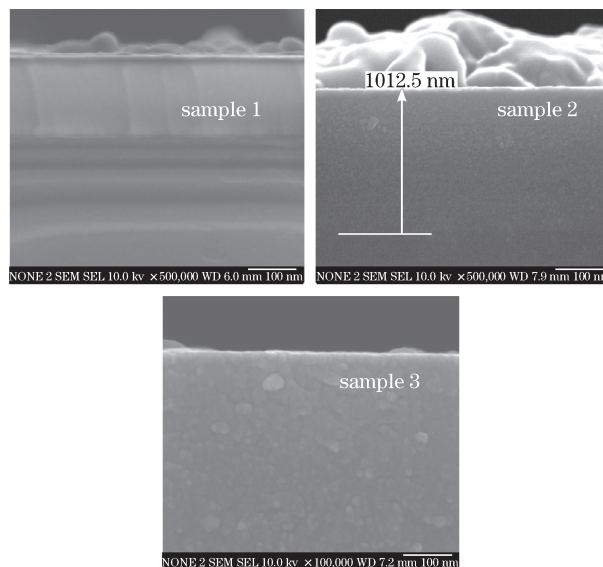


Fig. 8. Microstructures of the sample surfaces.

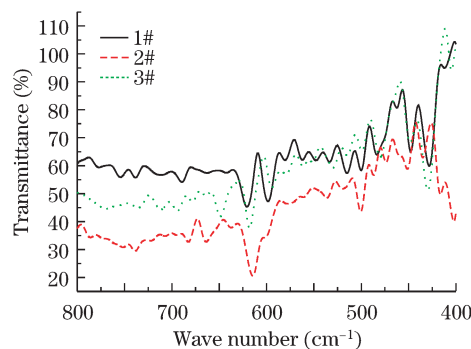


Fig. 9. Transmittance at IR (on silicon substrates).

between samples 1 and 2. The granule microstructure of sample 3 matches that of the EBED theory.

The experiment tested using an X-ray diffraction (XRD) instrument show that all the samples are amorphous films. Because the evolution of Al-O vibrations may give information about the Al-O network as well as the nature of the crystalline phase of alumina, the films are also analyzed by IR spectroscopy to detect the crystalline phase of alumina in the coatings<sup>[9]</sup>.

Sample 1 is presumed to be dominated by amorphous phase alpha  $\text{Al}_2\text{O}_3$  because there is obvious band at  $460\text{ cm}^{-1}$ , which is the characteristic vibration frequency of alpha alumina. But the inexact matching of the other two bands at  $690$  and  $530\text{ cm}^{-1}$ , which are related to gamma alumina, shows the disordered gamma phase. The minor absorptions at the three bands of sample 2 indicate a disturbance of its phase. The results of sample 3 demonstrate that gamma alumina should be expected in its composition.

In conclusion, the alumina coatings are applied using three different techniques, and the refractive index, absorption, roughness, and microstructure of the coatings are achieved. The coating produced by IBSD exhibits higher refractive indices, and it has the highest absorption in the UV region while the refractive index changes

gradually. Compared with IBS technique, EBED technique does not possess a great disparity with regards to alumina coating roughness. The IBS-deposited alumina coatings are dominated by the alpha alumina phase, whereas the EBED-deposited ones are dominated by the gamma alumina phase.

### References

1. S. Shang, C. Liao, K. Yi, D. Zhang, Z. Fan, and J. Shao, High Power Laser and Particle Beams (in Chinese) **17**, 511 (2005).
2. G. Liao, D. Ba, L. Wen, S. Liu, and S. Yan, Vacuum (in Chinese) **44**, 32 (2007).
3. Synthetic Sapphire, TYDEX, J. S. Co. <http://www.tydex.rµ>.
4. S. Novak, R. Hrach, J. Pavlik, and V. Hrachova, SPIE **2780**, 76 (1996).
5. J. C. Manificier, J. Casiot, and J. P. Fillard, J. Phys. E **9**, 1002 (1991).
6. T. Liang, *Physical Optics* (in Chinese) (2nd edition) (China Machine Press, Beijing, 1987).
7. R. Götzelmann, H. Hagedorn, A. Zöller, A. Kobiak, and W. Klug, Proc. SPIE **5963**, 5963L (2005).
8. Y. Wang, Q. Li, and Z. Fan, High Power Laser and Particle Beams (in Chinese) **15**, 841 (2003).
9. A. Pillonnet, R. Brenier, C. Garapon, and J. Mugnier, Proc. SPIE **5249**, 657 (2004).